038

PERFORMANCE PREDICTION OF INLET BARRIER FILTER SYSTEMS FOR ROTORCRAFT

Nicholas Bojdo[1] & Antonio Filippone
The University of Manchester
Manchester M60 1QD
United Kingdom

ABSTRACT

This contribution addresses the performance of Inlet Barrier Filter Systems (IBF) for rotorcraft with respect to IBF Design. IBF are fitted to rotorcraft to extract potentially harmful particles from engine-bound air. However, whilst protecting the engine from erosion and other damage, installation of an IBF incurs a loss in static pressure that is of detriment to the engine's performance. The inherent pressure drop across an IBF can be curtailed somewhat by pleating of the filter surface, but phenomenological effects that arise in the flow at high pleat density limit the extent of this action. The result is an optimum pleat shape for a given filter medium in a given flow. This contribution investigates the optimisation process for IBF with respect to IBF performance, which is assessed through three identified factors: pressure drop, capture efficiency and filter holding capacity; and makes provision for IBF Design in order that the IBF may be of maximum benefit to the engine.

INTRODUCTION

Helicopters are required to operate in many challenging environments, but non pose a greater threat to the turboshaft engine than one rich in dust and sand. To protect against this threat, operators may opt to install an Inlet Barrier Filter (IBF) at the engine intake to separate foreign particles from inbound dust-laden air.

IBF are installed ahead of the engine inlet, as a retrofitted appendage or as an integral part of the intake system. In the latter case, the IBF may be blended with the airframe such as on the MD 500, or may be installed in the intake cavity before the engine such as on the Bell 206B. The occurrence of such arrangements is commonly found on existing light, single-engine rotorcraft, to which the devices are easily adapted; or are found on newly fabricated light and medium rotorcraft, in which case the IBF may be implemented during rotorcraft design. On larger rotorcraft, where more power is needed, engines are larger and more numerous, therefore more air is required to achieve the operating mass flow rate. As a result, IBF fitted to existing rotorcraft are often bulky and conspicuous. An example is an IBF designed for the Sikorsky Blackhawk UH-60 by inventors Steltzer and Newman in U.S. Patent 7192462 [1], as shown in Fig. 1.

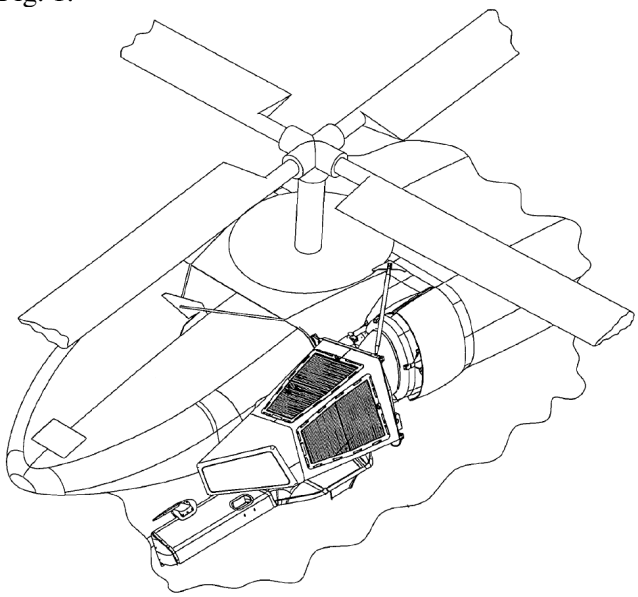

Fig. 1: IBF for Sikorsky UH-60 Blackhawk, according to U.S. Patent 7192462 [1].

The drag and weight penalty of an IBF device is offset by its ability to prolong the lifetime of an engine, by preventing the ingestion of particles that may otherwise erode compressor blades or cause glazing on combustor walls, causing a loss of performance. During brownout conditions, in which a helicopter is exposed to dust concentrations of 1.78 grams per cubic metre of air [2], an engine such as the Lycoming T55 may ingest over one kilogram of particulate per second[2]. The effect of this was perhaps best exemplified in the first Gulf War, when US Army CH-47 helicopters operating with no protection required engine replacements after as little as 25 hours of flight, due to the rapid erosion of engine turbine blades [3]. With current IBF purportedly being capable of removing 99% of AC Fine Test Dust, it would seem that installation of this device is unchallengeable. However, as with all aspects of aerospace engineering, nothing is for free.

Aside from the obvious weight and drag penalties, the other main side effect of IBF installation is a reduction in potential engine performance. There are two main causes for this: the first is flow distortion at the engine inlet as a result of the disturbance caused to the air flow by the filter, which can lead to compressor blade stall; the second is a drop in static pressure at the engine inlet, as the engine works harder to overcome energy losses across the filter. It is the latter of these that provides the main focus of the

[1] School of MACE, George Begg Building. Corresponding Author. Email: Nicholas.Bojdo@postgrad.manchester.ac.uk

[2] Based on engine mass flow rate of 27.4 lb/sec (12.4 kg/sec)

present work. By investigating the factors affecting pressure loss, we can assess the IBF performance and establish to what extent installation of such intake protection is beneficial to the engine.

Factors Affecting IBF Performance

An IBF system consists of one or more panels containing a filter medium sandwiched between two wire meshes. The filter medium is most often a *woven fabric filter* composed of a multi-layer cloth of criss-crossed yarns, but may also be a *fibrous filter* consisting of a bed of randomly assorted fibres. Particles are captured either on the surface of the filter (surface filtration) or are intercepted within the filter medium (depth filtration). The filter is removed and cleaned approximately every 100 hours, and replaced after 10 to 15 cycles. Frequency of cleaning may increase when conditions demand so; in any case the pressure drop across the filter is constantly monitored to support changes to the stipulated maintenance schedule. The filter is pleated to increase its surface area and improve rigidity, and is housed in a frame to be moulded into an intake or combined with other panels to form a filter box, as in Fig. 1. A graphical exemplar of an IBF is given in Fig. 2.

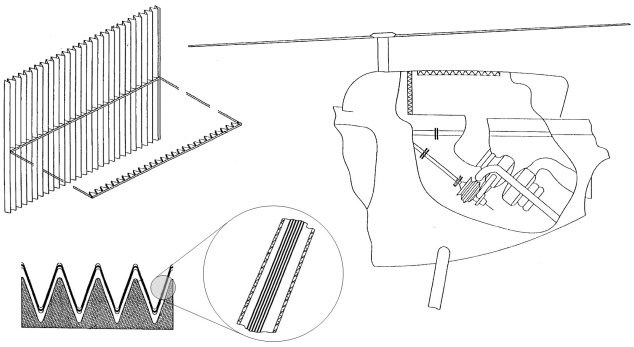

Fig. 2: Example of pleated filter for IBF application, according to U.S. Patent 6595742 [4].

The performance of an IBF system is not a simple matter. To ease assessment, we have singled out four key areas for investigation that separately affect the overall pressure drop across the filter. They are:

1. *The Filter Medium* – The material of which the porous matrix is composed.
2. *The Cake* – The term appropriated to the layer of particles accumulated on the surface of the filter.
3. *IBF Design* – The way in which the filter is constructed to achieve the desired results.
4. *IBF Integration* – The way in which the filter is installed into the airframe.

By understanding greater the contribution of each constituent, we can establish the factors that determine the overall performance of the IBF and ultimately, the effect of its presence on the engine. It is the third area that represents the focus of the current work. The first two areas have been investigated in a previous study; the fourth will be the subject of a future study.

With regard to the filter medium, previous work found that the collection efficiency of a given fabric (the proportion by volume of particles removed from the air) is highly dependent on the filter cloth and particle properties. It was found that the efficiency of a given filter varies as a function of particle size: particles of diameter larger than the yarn spacing are immediately blocked; medium sized particles that permeate the first cloth layer may be arrested later by a yarn in the adjacent layer; the smallest particles follow the tortuous fluid streamlines between and through the spun-fibre yarns, and may be picked up by loose fibres. To model this we idealise the multi-layer cloth as a homogeneous depth filter, and use established empirical formulae to predict the likelihood of a particle of a certain diameter being captured by a given cloth. This yields a *capture efficiency profile* for the fabric cloth, for a range of particles usually between 0.1 and 1000 μm. This can be improved by increasing the yarn diameter, yarn density (mass of fibres per unit length of yarn) or warp-weft density (number of yarns per unit area of cloth), which all serve to increase the filter packing fraction (solid proportion of filter volume). However, such measures also increase the pressure drop across the clean filter.

The pressure drop across any porous medium is related to the porosity, or volume of empty space within the porous matrix. As porosity decreases, the ability of the medium to transmit fluid, or the filter permeability, also decreases. For cloth filters, the porosity is the opposite of the packing fraction. Any particles that are captured within the cloth serve to lower its porosity as pore spaces are filled up, which means the pressure drop is in a transient state of incline. This warrants regular cleaning of the filter, which can be difficult if all the particles are trapped inside the filter bed. To lengthen the lifetime of the filter, the medium can be constructed to encourage more interception at the surface of the filter, allowing the collected particulate cake to be dusted off during maintenance. An additional benefit is that the cake also acts as a filter, as large particles lying in a layer on the surface can trap smaller particles in their interstices. This type of filtration is known as surface filtration, and is more common in hydrological applications such as water purification. IBF utilise both depth filtration and surface filtration: the former captures smaller particles and dictates the lifetime of the filter; the latter captures larger particles and augments the filtration process, while mainly dictating the maintenance schedule. The significance of the surface cake therefore cannot be understated.

It is the contribution to overall pressure drop of the surface cake that provides the stimulus for investigation. It was found in earlier work that cake accumulation is a complex phenomenon to model,

thanks in part to the wide range of particle shapes, sizes and densities that are common in most slurries, especially a sand-laden fluid. Additionally, it was found that as the cake builds up, the particles closest to the filter surface are put under increasing pressure by the drag force of the particles stacked above. This manifests itself as compaction, which is experienced throughout the cake in varying amounts depending on proximity to the surface, and leads to the formation of an inhomogeneous cake. The result is a depth-wise variation in porosity and thus a depthwise variation in pressure drop. To complicate matters further, the degree of compaction is different for all materials: sand (of which there are many types alone) may compact much more quickly than chalk, but may reach a higher minimum porosity. Such behaviour can be predicted with so-called empirically-derived *compaction coefficients*, which allow the pressure drop to be estimated for a given particle volume feed rate, but the complex nature of cake build-up must be regarded in the applicability of such models.

The effect of the cake on IBF performance may be dwarfed by the contribution of the IBF Integration. The position of the IBF relative to the rotor may affect the inflow conditions, while orientation to the incident airflow may affect the number of particles reaching the filter. However, it is the objective of the present work to investigate the effect on performance of IBF Design.

IBF DESIGN

The construction of the filter is paramount to its effectiveness. We have identified three *performance factors*, which act as drivers for IBF design. They are:

1. *Pressure Drop* – The loss in static pressure of the influent air as a direct result of IBF installation. The lower the pressure drop, the less adverse the performance loss to the engine.
2. *Capture Efficiency* – The proportion of particles removed from the dust-laden air by the filter. The higher the capture efficiency, the less the risk of damage to the engine by dust particles.
3. *Holding Capacity* – The volume of filter per unit span, or the potential ability of a filter to retain particles. The higher the holding capacity, the longer it takes to become clogged, thus the longer the lifetime of the filter.

Determination of the three drivers is made complicated by the numerous variables involved. To aid discussion of these, it is useful to employ a flowchart, as given in Fig. 3. As can be seen, the ultimate reference point in this design process is the engine – in what way will the IBF affect the engine, and what can be done to minimise costs while maximising benefits. Next are the factors that are pre-determined: the engine position in the airframe, the required engine mass flow rate, and the particle properties. These provide the initial conditions with which an IBF is designed.

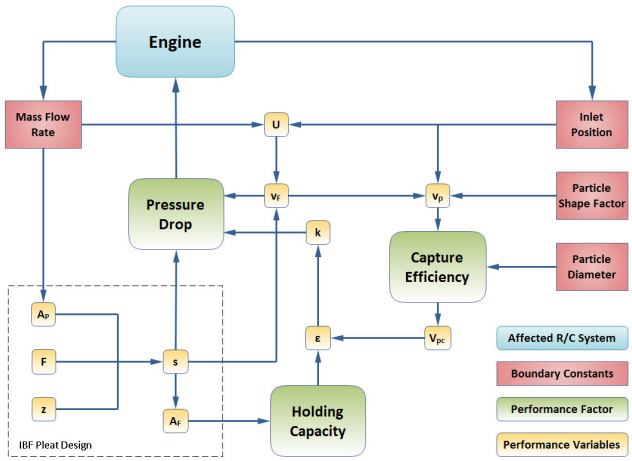

Fig. 3: Factors affecting IBF Performance.

Aside from the filter medium itself, the other key filter design variable is the construction of the pleats. A filter is pleated to increase its surface area, which lowers the filter face velocity and increases the total filter volume, providing benefits to all three performance factors. A lower face velocity results in less viscous and inertial losses from the fluid as it passes through the filter, thus reducing porous medium pressure loss. It also slows down particles entrained in the streamlines, which increases their likelihood of being intercepted and therefore raises the capture efficiency. Increasing the filter surface area also provides more space within the filter to hold captured particles, which prolongs the lifetime of the filter by reducing the rate of increase of filter porosity thereby slowing the pressure drop rise.

The flowchart illustrates the additional connections between each performance factor and highlights the most influential variables. To demonstrate how each variable is linked, we begin with the boundary constants of Inlet Position and Mass Flow Rate, which determine the approach velocity U of the influent air and coupled with the particle properties, the velocity of the particulates, v_P. Assuming the filter fabric properties are fixed, this determines the Capture Efficiency of the IBF, which then gives us the quantity of particles extracted from the air. The filter surface area per unit span gives us a measure of the Holding Capacity, which is combined with the influx volume of particles to determine the rate of decrease of filter porosity, $d\varepsilon/dt$ and therefore decrease of filter permeability, dk/dt. A lower permeability induces greater loss of energy to viscous effects, which is tapped from the static pressure. The Pressure Drop across the filter is also related to the filter face velocity v_F, which itself depends on the influent velocity U, the filter surface area A_F and the

pleat shape, which brings us back to the boundary constants and the pleat construction.

Pleated Filter Design

Given the phenomenological effects of pleating a filter, it would seem logical to employ as many pleats as possible. However, studies have shown that as the pleat count (pleats per unit length) increases, an additional source of pressure loss arises. A study into the optimisation of pleated filter designs by Pui Da-Ren-Chen *et al.* [5] reports that while the reduction in face velocity lowers the filter medium pressure loss, as the number of pleats begins to increase, so does the viscous drag at the flow-media interface. In addition to this, the increased pleat crowding enhances flow contraction upstream of the filter, and flow expansion downstream of the filter, which further extracts energy from the flow. These effects result in an increase in pressure drop at a high pleat count. The consequence is an optimal pleat count for a given filter thickness, permeability and pleat height, which occurs when the combination of viscous drag and media resistance is at a minimum.

In a separate study, Subrenat *et al.* [6] contest that a side effect of increasing pleat count is an overlapping of the filter media at each fold, which reduces the effective cross section available to the flow. If pleat count continued to increase, the filter would eventually resemble a solid homogeneous structure of thickness equal to the pleat depth, and the fluid would flow only through the head of the pleat. This would raise the pressure drop considerably. This is supported in a study by Wakeman *et al.* [7], in which a simulation is performed on a pleated cartridge filter typically used in the filtration of hydraulic fluids for aeronautical applications. While the filtrate and operating pressure differ greatly from the application discussed in the present study, the conclusions drawn can be applied. Wakeman *et al.* found that the effects of pleat crowding and pleat deformation contributed to a loss in filtration area, which increased with number of pleats. Furthermore, the effect of material folding was seen to compress the material (depthwise) through spanwise tension, and thus lower the local permeability at a location through which a larger proportion of fluid flows. The consequence of these pleating effects is a further increase in pressure loss.

Such phenomena again illustrate the search for the ideal pleat shape. However, given the dependence of the pressure drop on other factors such as filter permeability and approach velocity, it is likely that during lifetime of the IBF, the optimum pleat shape will differ from the one for which it was designed. The design process may therefore consider the effect of the pleat shape on the other two performance factors. For instance, given that the filter porosity will decrease with operation time, perhaps it is worth increasing the pleat count beyond the optimum, in order that the holding capacity is increased and the transient pressure drop rises at a lower rate. Likewise, since a low face velocity favours the capture of the smallest particles, perhaps it is worth sacrificing a higher pressure drop to improve the collection efficiency. To begin an investigation into such questions, we perform a parametric study on typical pleat shapes for IBF, using flow conditions that may be experienced during operation.

Parametric Study of IBF Pleat Design

The parametric study is conducted using CFD software in two dimensions, and has three objectives:

1. To investigate the effect of pleat size and pleat shape on pressure loss.
2. To investigate the effect of approach velocity and pleat shape on pressure loss.
3. To investigate the effect of filter permeability and pleat shape on pressure loss.

The simulations are carried out on a single pleat of rectangular construction, which is an idealised interpretation of the triangular-shaped pleat with rounded folds that is more typical of pleated filters. Earlier simulations with a purely triangular configuration were deemed unsatisfactory when a high pleat count was tested, due to high medium density at pleat folds. More accurate would be a triangular shape with rounded folds meaning a gentle blending of one pleat into the next, however for a parametric study requiring numerous different shapes, such a configuration would be too time-consuming to construct. A typical idealised rectangular pleat is shown in Fig. 4.

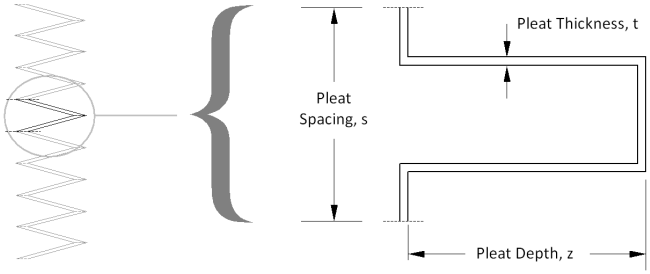

Fig. 4: Idealised Pleat Configuration for CFD Analysis.

The pleat shape is varied by altering the non-dimensional pleat shape factor F, defined as the spacing s divided by the depth z, for different pleat counts. The pleat count is defined as the number of pleats per unit length, which is simply the inverse of the pleat spacing. For example, a pleat shape factor of 0.5 for a pleat count of 0.25 pleats per centimetre gives a pleat with a spacing of 40 mm and a depth of 80 mm. For clarity, the smaller the pleat shape factor, the more elongated the pleat; while the smaller the pleat count, the larger the span of the pleat. According to U.S. Patent 6595742, which refers to an IBF system devised by Scimone [4], a typical pleat depth range is 1 to 3 inches (25 to 75mm) and a typical pleat density is 2 to 6 pleats per inch (0.787 to 2.362 pleats per centimetre).

These provide the typical dimensions around which to base the investigation.

For the investigation into the effect of pleat size, we test four different pleat counts (from 1.0 to 0.1 pleats per centimetre) across the same range of 6 pleat shape factors (from 0.125 to 4). For the investigation into the effect of velocity, we test one pleat count set (of 6 shape factors) for 3 different approach velocities, from 1 ms^{-1} to 10 ms^{-1}. For investigation into the effect of permeability, we test one pleat count set for three different coefficients of permeability. In all tests, variables not being investigated are held at pre-determined default values, which in the absence of real case data are based on typical values for this application. For example, the filter thickness (2 mm) is based on a 6 layers of 0.33 mm thick cotton filter cloth, with typical packing fraction of 25% and permeability 6 E-10 m^2. The pressure drops are non-dimensionalised with the pressure drop across an unpleated (flat) filter of equal thickness and permeability in identical flow conditions.

Computational Flow Modelling through Porous Media

To perform a parametric study on IBF design, we use the Computational Fluid Dynamics (CFD) software *Fluent* to model flow through a pleated filter. Fluent models porous media by adding a momentum source term to the standard fluid flow equations. This is applicable only to the area or volume specified by the user to represent the porous medium in two or three dimensions, respectively. The source term has two constituents: a viscous loss term, and an inertial loss term. These loss terms represent a momentum sink that contributes to the pressure gradient across the medium, creating a pressure loss. For homogeneous porous media, the sink term is written

$$S_i = -\left(\frac{\mu}{k} v_i + \frac{1}{2} Y \rho v_{mag} v_i \right) \qquad (1)$$

where the terms k and Y represent respectively the permeability coefficient and inertial resistance factor, while v and μ are velocity and viscosity respectively. The inertial term caters for non-linear effects through the porous medium, which according to Miguel [8] have been experimentally observed when the Permeability Reynold's Number ($Re_k = \rho v k^{-1/2}/\mu$) exceeds unity. However, while Re for the test velocities and permeabilities is in the range of approximately 1 to 40, preliminary simulations exhibited a linear pressure gradient through the porous media, therefore the inertial losses can be assumed to be negligible. This negates the term on the right hand side of Eq.1.

Preliminary simulations were also carried out to establish grid independence, which occurred at a grid size of around 900,000 cells. The flow is considered steady, isothermal, incompressible, axisymmetric and turbulent. The classical k-ε model is used to account for turbulence. A turbulence lengthscale of 7% of the pleat width was used, and an assumed turbulence intensity of 3% was deemed suitable for this application.

RESULTS

The figures below display the results from the three investigations. Figs. 5-6 show the absolute and non-dimensionalised pressure drops for 4 ranges of pleat shape. Recalling that a smaller pleat shape factor reflects a more elongated pleat, it appears that for a given pleat count, there appears to be an optimum pleat shape for minimum pressure loss. This is the classic trend observed by other studies in pleated filters. Furthermore, as pleat count decreases, the optimum pleat shape becomes more elongated, and the pressure drop becomes smaller.

The effect of approach velocity U on resulting pressure drop across a pleated filter, is shown in Figs. 7-8. Six pleat shapes of equal width (40 mm corresponding to a pleat count of 0.250 pleats/cm) are subjected to velocities of 1 ms^{-1}, 5 ms^{-1} and 10 ms^{-1}. It is evident from Fig. 7 that an increase in velocity results in a higher pressure drop across the filter. However, the increase is not linear. For example consider a pleat with a shape factor of 1. For a pleat spacing of 40 mm, this corresponds to a pleat depth of 40 mm. At 5 ms^{-1} the pressure drop is approximately 200 Pa, but when the velocity is doubled, this rises to around 500 Pa. We also see from Fig. 8 that the optimum pleat shape for minimum pressure drop drifts to a deeper pleat with decreasing velocity.

The results from the third investigation, which examined the effect of permeability on pressure drop, are displayed in Figs. 9-10. Here we see that decreasing a filter's permeability causes the pressure drop across a pleated filter to increase disproportionately. We also see that the optimum pleat shape for minimum pressure does not change dramatically, shifting slightly towards a less elongated pleat with decreasing permeability. Another interesting trend apparent in Fig. 10 is that pleating has a more significant effect on reducing the relative pressure drop when the filter permeability is low, than when the filter is more permeable.

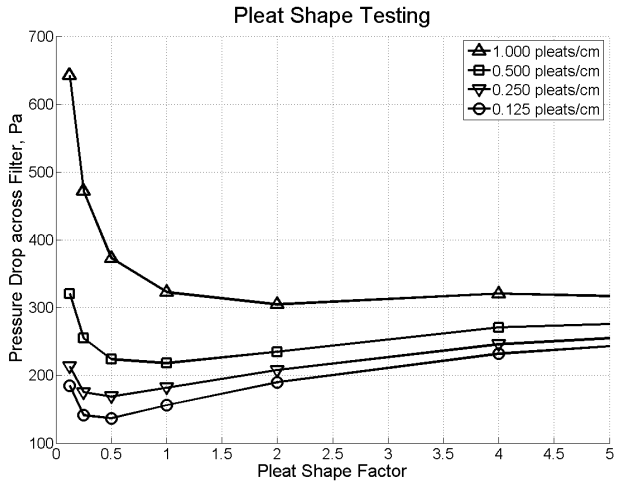

Fig. 5: Effect of Pleat Shape Factor and Pleat Count on Pressure Drop.

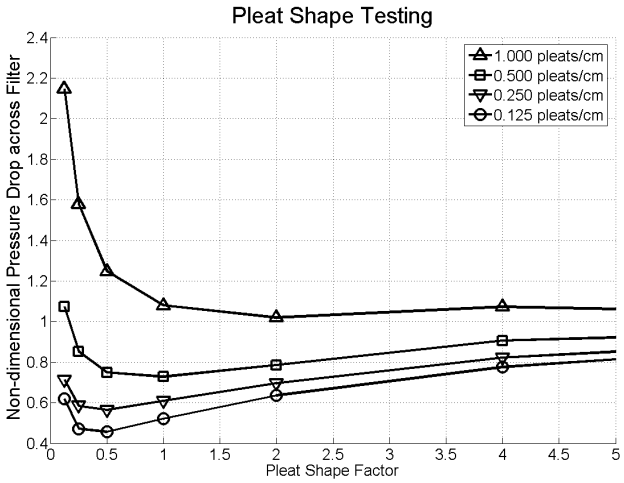

Fig. 6: Effect of Pleat Shape Factor and Pleat Count on Non-dimensionalised Pressure Drop.

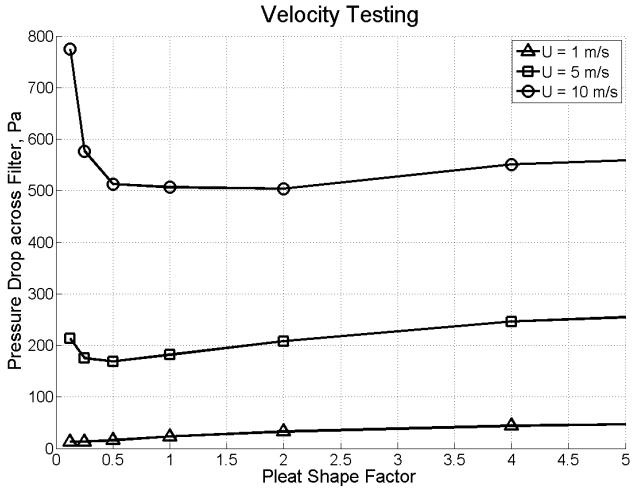

Fig. 7: Effect of Approach Velocity on Pressure Drop.

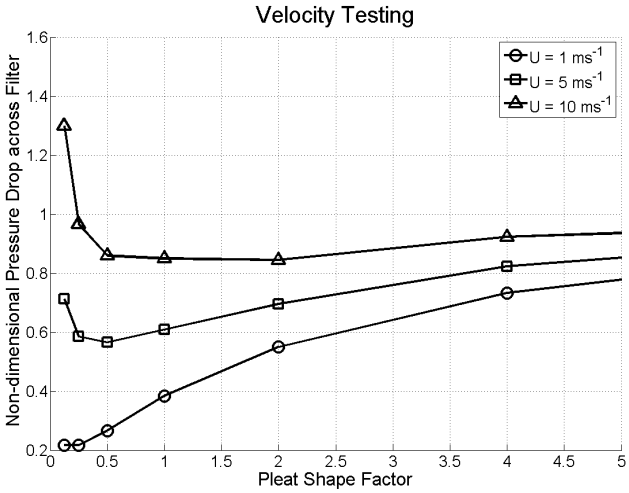

Fig. 8: Effect of Approach Velocity on Non-dimensionalised Pressure Drop.

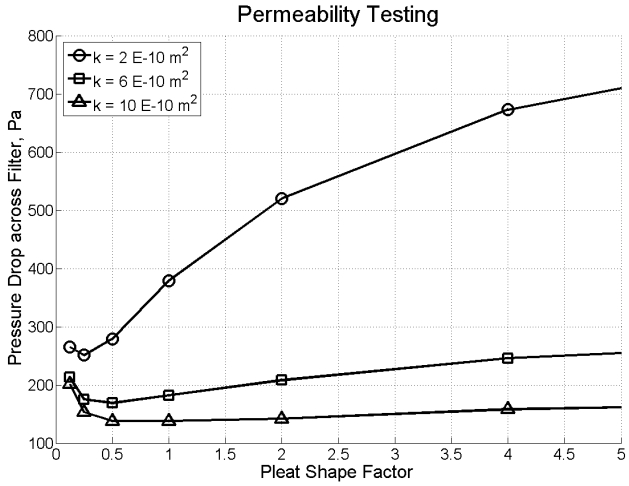

Fig. 9: Effect of Filter Permeability on Pressure Drop.

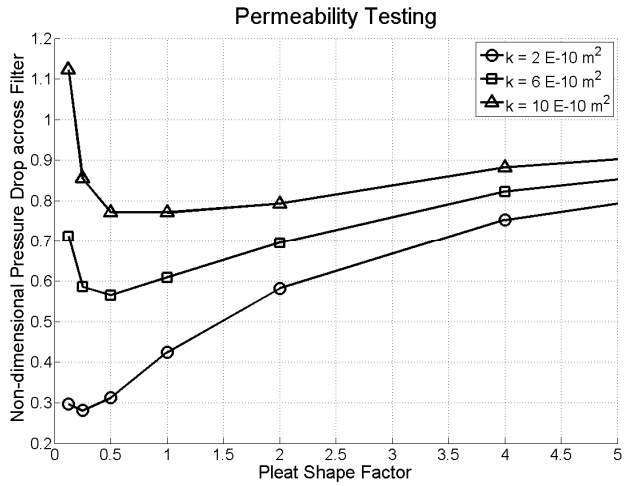

Fig. 10: Effect of Filter Permeability on Non-dimensionalised Pressure Drop.

DISCUSSION

The observed, classic U-shape that is synonymous with pleated filter analysis occurs due to a variation in dominance of the two contributors to pressure loss. In general, decreasing the pleat shape factor results in an initial reduction in the pressure drop across the filter, but at a certain point, the pressure begins to rise again. The first investigation examines how this optimum point changes with pleat geometry, for a given filter permeability, thickness and given approach velocity. It is found that as pleat count increases (or pleat spacing decreases) the optimum pleat shape is found at a larger pleat shape factor. Put differently, the pressure drop across a given pleat shape is dependent upon the pleat's absolute size. The pressure drop across a smaller pleat is large, because the gap between each pleat is smaller. This causes a greater degree of contraction, leading to increased velocity within the gaps and an increased loss to flow shear stress. The subsequent expansion on exiting the leeward gap, which is more extensive for a smaller pleat, also extracts energy from the air. This is evident in Figs. 11 and 12, which show the magnitude of the flow velocity around pleats of identical shape but different size. (Fig. 11: U_{max} = *15.0* ms^{-1}; Fig. 12: U_{max} = *11.5* ms^{-1}).

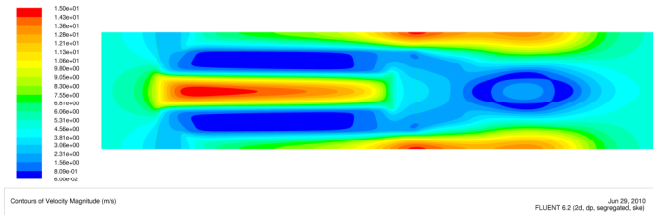

Fig. 11: Velocity Magnitude distribution across pleat of Shape Factor 0.5 and pleat spacing 10 mm (pleat depth: 20 mm).

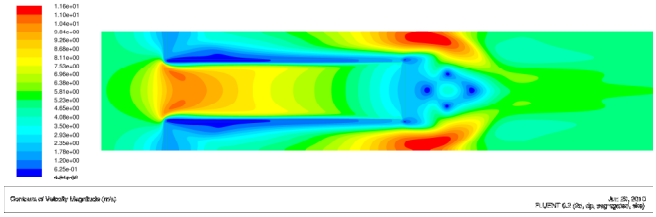

Fig. 12: Velocity Magnitude distribution across pleat of Shape Factor 0.5 and pleat spacing 100 mm (pleat depth: 200 mm).

The results from the velocity testing and permeability testing can be explained similarly. Regarding the effect of increasing velocity, the pressure loss is greater thanks to both increased viscous loss through the filter and increased flow contraction and expansion. However, we also see that an increase in pleat depth is far more effective at low approach velocity, than at high velocity. The migration of the optimum pleat shape to a higher shape factor at higher velocity suggests that as the approaching flow rate increases in magnitude, the loss of energy to fluid shear stress becomes more dominant. In fact, at a velocity larger than 10 ms^{-1}, the effect of pleating may be of detriment to the pressure drop rather than of benefit.

The effect of decreasing the filter permeability is to increase the pressure drop across the filter. This is because the permeability is a measure of the ability of a porous medium to transmit fluid; a lower permeability means a lower porosity, which means more energy lost to frictional effects. Figs. 9 and 10 also show that as permeability decreases, the optimum pleat shape drifts towards a more elongated pleat. This is exemplary of an increasing contribution of filter medium pressure loss, a fact that serves to enforce the previous explanation.

CONCLUSIONS

Given the numerous estimates of typical values that have been used in this study (due to an absence of real data) it would perhaps be unwise to dwell on exact values for pressure drop across a pleated filter for IBF. However, the trends recognised in the results of the investigation mirror those found in other studies in pleated filters (see Pui Da-Ren Chen *et al.* [5], Chen *et al.* [9], Lücke & Fissan [10]) and provide useful information in further understanding the importance of pleat design in determining IBF performance.

An investigation into the effects of approach velocity on resultant pressure drop has revealed that the optimum pleat shape for minimum loss is not static. Therefore designers may wish to size IBF pleats according to a pre-calculated average approach velocity in order to maximise performance, whilst also being aware that high velocity flow may even negate the requirement for pleats. This may require an understanding of the flow field around the airframe to establish the nature of the inbound air. For example, an IBF located directly beneath the rotor disk may be designed differently to one place on the side of the airframe, due to the influence of the downwash.

As the filter collects particles from the air, its porosity decreases, leading to a decrease of permeability. Given the large impact of a decrease in permeability, designers may wish to sacrifice a higher initial pressure drop with a larger pleat count or pleat depth in order to increase the filter holding capacity and thus slow the fall in porosity. Knowledge of the filter medium structure and the sand type to be captured could be combined with these conclusions to predict the transient performance of an IBF and provide further education to the optimisation process.

The investigation into pleat shape revealed that the optimum shape becomes more elongated with decreasing pleat count. However, in order to enhance assessment of optimum pleat shape, it is useful to display the results in a different way. Fig. 13 shows the

variation in pressure drop with pleat count, for four separate pleat depths.

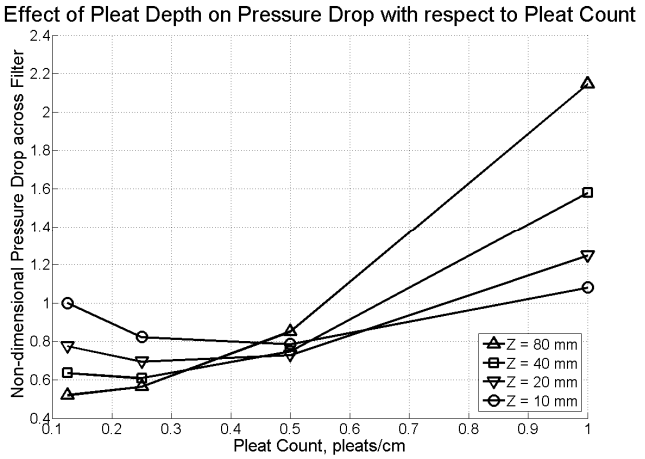

Fig. 13: Pressure drop across a pleated filter as a function of pleat count for four pleat depths.

In addition to exhibiting the classic U-shape for all series, Fig. 13 also illustrates the effect of increasing pleat depth on pressure drop. The left hand side of the U-shape corresponds to pressure loss dominated by the filter medium; the right hand side corresponds to loss dominated by flow contraction and expansion. An increase in pleat depth appears to exacerbate the pressure loss when the pleat count is high, but alleviates it when the pleat count is low. The classic U-shape seems to almost tip to the left or right depending on whether the pleat depth is increased or decreased respectively, about a pivot point at approximately 0.5 pleats per centimetre. The fulcrum of this see-saw is unique to a given filter medium in a given flow and represents the pleat count at which changes to the pleat's depth have the least effect on pressure drop. This could be useful in the optimisation process when combined with the other conclusions drawn from this study. Holding the pleat count at this value, pleat depth could be adjusted to cater for predicted changes to the filter permeability or approach velocity, whilst knowing that the IBF is working at its maximum performance potential when average values are assumed.

This study has highlighted the contributing factors to the performance of IBF for helicopters. In particular it has investigated the components of IBF Design, and examined the effects of altering filter pleat geometry on pressure drop. The conclusions drawn from the variable optimum design point can be combined with the other areas of IBF analysis to establish the overall performance of a barrier filter and ultimately, the effect of its presence on the engine.

NOMENCLATURE

ε = filter porosity
A_F = filter surface area, m^2
A_P = IBF profile area (intake profile area), m^2
F = pleat shape factor
k = filter permeability, m^2
s = pleat spacing (pleat width), mm
U = approach velocity, ms^{-1}
V_{PC} = collected particulate volume, m^3
v_F = filter face velocity, ms^{-1}
v_P = particle velocity, ms^{-1}
Z = pleat depth, mm

μ = dynamic viscosity, $kgms^{-1}$
S_i = momentum sink, $kgms^{-2}$
v_i = local flow velocity, ms^{-1}
v_{mag} = local flow velocity magnitude, ms^{-1}
Y = inertial resistance factor, m^{-1}

REFERENCES

[1] J.F. Stelzer and T.L. Newman, *Engine Air Filter and Sealing System*, U.S. Patent 7192462, March 20, 2007.

[2] M.E. Taslim and S. Spring, *A Numerical Study of Sand Particle Distribution, Density, and Shape Effects on the Scavenge Efficiency of Engine Inlet Particle Separator Systems,* Journal of the American Helicopter Society, vol. 55, Apr. 2010, pp. 022006-9.

[3] P. Stallard, *Helicopter Engine Protection*, Perfusion, vol. 12, issue 4, July 1997, pp. 263 - 267.

[4] M.J. Scimone, *Aircraft Engine Air Filter and Method*, U.S. Patent 6595742, July 22, 2003.

[5] D.Y.H. Pui Da-Ren Chen and B.Y.H. Liu, *Optimization of pleated filter design using a finite-element numerical method*, Journal of Aerosol Science, vol. 24, issue suppl. 1, 1993, pp. S39-S40.

[6] A. Subrenat, J.N. Baléo, and P. Le Cloirec, *Analysis of pressure drops in pleated activated carbon cloth filters*, Journal of Environmental Engineering, vol. 126, Jun. 2000, pp. 562–568.

[7] R.J. Wakeman, N.S. Hanspal, A.N. Waghode, and V. Nassehi, *Analysis of pleat crowding and medium compression in pleated cartridge filters*, Chemical Engineering Research and Design, vol. 83, Oct. 2005, pp. 1246–1255.

[8] A.F. Miguel, *Airflow through porous screens: from theory to practical considerations*, Energy and buildings, vol. 28, Aug. 1998, pp. 63–69.

[9] C.W. Chen, S.H. Huang, C.M. Chiang, T.C. Hsiao, and C.C. Chen, "*Filter quality of pleated filter cartridges*, Annals of Occupational Hygiene, vol. 52, Apr. 2008, p. 207.

[10] T. Lücke and H. Fissan, *The prediction of filtration performance of high efficiency gas filter elements*, Chemical Engineering Science, vol. 51, Apr. 1996, pp. 1199-1208.